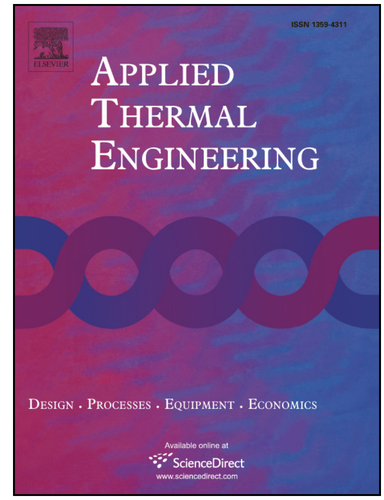

Research Paper

Optimization of thermal design and geometrical parameters of a flat tube-fin adsorbent bed for automobile air-conditioning

M. Verde, K. Harby, José M. Corberán

PII: S1359-4311(16)31769-0
DOI: http://dx.doi.org/10.1016/j.applthermaleng.2016.09.099
Reference: ATE 9124

To appear in: *Applied Thermal Engineering*

Received Date: 9 June 2016
Revised Date: 18 September 2016
Accepted Date: 19 September 2016

Optimization of thermal design and geometrical parameters of a flat tube-fin adsorbent bed for automobile air-conditioning

M. Verde[a], K. Harby[a,b,*], José M. Corberán[a]

[a]Instituto de Ingeniería Energética, Universidad Politécnica de Valencia, Camino de Vera 14, ES 46022 Valencia, Spain

[b]Mechanical Power Engineering and Energy Department, Faculty of Engineering, Minia University, 61519, Minia, Egypt

[*] **Corresponding author:** +2 01060204458; fax: +2 086 2346674

Email: khaledharby8@yahoo.com

ABSTRACT

Adsorbent bed design and performance strongly affect the overall performance of adsorption systems. In the present study, an analytical model was developed to determine the optimum geometrical and thermal parameters of a flat tube-fin adsorbent bed to reach the maximum system performance. This types of heat exchangers offer substantial reduced in weight, cost, volume and thermal conductivity, which can make them a good choice for adsorbent beds in automobile applications. Results showed that the overall thermal conductance of the bed and the maximum practical specific cooling capacity increased when reducing in flat tube thickness and fin pitch as well as by increasing in fin thickness and water channel wall thickness. The specific thermal conductance increased by 2.5% when reducing the channel pitch from its design value to a minimum permissible (0.004m). From thermal parameters that have been studied, the adsorbent thermal conductivity is the most sensitive parameter to the specific thermal conductance in beds. The system performance also significantly enhanced by reducing the mass of the metal

bed and the heat transfer fluids as well as the desorption heat of the selecting working pair.

Keywords: Adsorption chiller, flat tube-fin heat exchanger, optimization, waste heat recovery, automotive A/C system, extended surface.

1. Introduction

Reduction of energy consumption by reducing the consumption of energy services and through efficient energy usage is turning out to be one of the important topics nowadays [1]. Research activity on thermally driven adsorption systems has received much attention in the recent years. Adsorption systems can be driven by waste heat and low-grade heat source (<100 ºC) and they use environmentally friendly refrigerants such as ammonia or water [2, 3]. In addition to environmental benefits and energy saving, these systems have many other advantages such as lack of moving parts, low operating costs, vibration-free operation and simple control [4, 5]. These features make them suitable for applications in automotive air conditioning systems using waste heat from the engine operation without losing mechanical energy, which can also reduce the carbon footprint [6].

However, the major drawbacks of adsorption systems are their low energy efficiency (COP and SCP), large size and mass and high investment costs when compared to conventional systems. These drawbacks prevent adsorption systems from commercialization and widespread utilization, especially in automotive applications [7, 8]. Good heat transfer performance in adsorbent beds increases the total heat transfer coefficient and the rate of heat transferred between the adsorbent and the heat transfer fluid [9]. In a similar view, good mass transfer performance will reduce the diffusion time of the adsorbate in the adsorbent and shorten the cycle time, which will then cause an increase in overall system performance [10].

Therefore, the need for efficiency improvement of adsorption systems encourages scientists to search for possibilities of improving heat and mass transfer in the adsorbent beds during adsorption-desorption cycles. Most of searches focused on adsorption properties of adsorbent/adsorbate pairs, adsorption/desorption cycles, and design modification of the adsorbent bed [11]. Different types of heat exchangers are used in adsorbent beds such as plate-finned tubes, and a capillary tube bundle HE [12], a flat-plate type HE with fins [13], a serpentine flat-pipe HE, and spiral plate HE [14]. Many researchers have proposed various types of sorption bed designs in order to enhance the heat transfer rate in the adsorbent bed [15-22].

Verde et. al [23, 24] studied theoretically and experimentally the performance of a proposed silica gel adsorption system for automotive air conditioning system. A flat tube-fin heat exchanger was used as an adsorbent bed. An improved non-equilibrium lumped parameter model was developed to predict the dynamic performance of the system under different real driving conditions. Different design configuration and operation strategies had been carried out in order to explore further improvements of the system performance.

Results showed that, using two radiators in the system instead of one radiator increases the cooling capacity by 7.0% and decreases the cabin temperature by 9.1 %.

There is relatively limited information regarding the effect of adsorption bed geometrical parameters with fins on the systems performance. Rezk [25] studied theoretically the effect of various adsorbent bed heat transfer enhancement techniques on the performance of a two-bed adsorption chiller. The results showed that cooling capacity and COP increased with increasing the fin spacing ratio to reach maximum of 25 % and 10 % respectively at fin spacing ratio of 2. Hamid et. al [26] developed a transient two-dimensional model for adsorption bed with annular fins to study the effect of bed configuration on the system performance. They showed that the COP of the cycle is slightly influenced by the fins number and strongly dependence on the fins height. Niazmand et. al [27] developed a three-dimensional model for adsorbent bed with square and annular plate fins. They showed that the cooling capacity can be increased by the increase of the number of fins and the decrease of the fins height. In addition, COP increases and SCP decreases with increasing fin height and fin pitch. Rezk et. al **[28]** developed a lumped analytical simulation model for silica gel/water adsorption system. They showed that the cooling capacity increased by 3% and the COP decreased by 2.3% when varying the fin spacing from its design value to a minimum permissible. Khan et al. **[29]** studied the effect of overall thermal conductance and adsorbent mass on the performance of a two-stage adsorption system. They found that system performance can be strongly influenced by the bed overall thermal conductance. Furthermore, they showed that the COP can be increased by the reduction of the adsorbent mass.

The literature review indicates that, many of these studies have proposed various types of bed designs. Few studies carried out on the effect of bed geometrical parameters on the heat transfer rate and hence how it affect the system performance. However, there was no information about the optimization of the thermal and design parameters in order to enhance the heat transfer rate and hence the overall system performance.

Therefore the purpose of the present study is to optimize the different parameters that mostly affect the performance of a flat tube-fin heat exchanger for automobile adsorption systems. An analytical model has been developed in order to estimate the overall thermal conductance of the heat exchanger by using a thermal resistance network. A parametric study was performed using the model to determine the effect of different bed parameters on the specific thermal conductance and maximum practical specific cooling capacity of the adsorbent bed. Physically, the proposed flat tube-fin heat is constructed by flat channel tubes covered with uniformly spaced flat fins to increase the heat transfer area on the air side which will be employed to increase the heat transfer to the adsorbent. They are available in the markets where used normally as evaporator in the conventional automotive air conditioning systems, therefore they are available at a low cost. In addition these type of HE are made from aluminum, have the advantages of low weight and low thermal capacity (lower heat losses) compared with other heat exchangers. The literature survey is relatively limited to this type of adsorbent bed. Therefore, further studied on these types are needed.

2. System description

Fig. 1(a) show a picture of the prototype adsorption chiller in the laboratory and fitted in a passenger vehicle Fig. 1 (b). The system description, components, and the working principle of the system, silica gel-water air conditioning adsorption system, has been described in detail in our previous work [22, 23]. The system was designed and tested under the framework of the TOPMACS project [30] for automotive air conditioning applications. As shown, the system consists of four heat exchangers namely, an evaporator, a condenser and two adsorber/desorber heat exchangers (Bed 1 and Bed 2).

Each adsorbent bed have three brazed type flat-tube fin heat exchangers connected in parallel as shown in Fig. 2. The heat exchangers are made from aluminum with brazed fins. Aluminum material enables the bed to operate at a lower temperature difference, reduce the weight of the system and provide high heat transfer efficiency. The weight of each aluminum heat exchanger (excluding the headers) is approximately 1.012 kg and the fin side of each heat exchanger is filled with 1 kg of silica gel grains. The heat transfer fluid selected for heating and/or cooling the bed is pure water.

3. Mathematical modeling

The heat exchanger is constructed by flat channel tubes covered with uniformly spaced flat fins to increase the heat transfer area on the air side. Fig. 3 shows the design parameters of the modelled flat-tube fin heat exchanger. Each channel tube comprises of two flat plates and an interplate channel, which carries the heat transfer fluid (i.e. water) for heating or cooling the packed adsorbent in a cyclic manner. The number of channels determines the total heat transfer surface. The geometrical parameters of the heat exchanger are detailed on Table 1.

The heat is transferred from the water to the adsorbent firstly, from the heat transfer fluid (hot or cold water) to the inner wall surface at $T_{s,i}$ by convection, with a convective heat transfer coefficient h_w. Secondly, across the plate by conduction with a thermal conductivity of k_{met}. Finally, from the outer wall surface at $T_{s,o}$ to the adsorbent at T_{ads} through two parallel heat flow paths: by conduction from the finned surface and by conduction from the unfinned surface.

3.1 Model assumptions

The assumptions considered in the present study are:

a) The thermal conductivity of the metal is constant,

b) The heat is transferred through the flat fins under one-dimensional conditions in the longitudinal (x) direction,

c) The base of the fins are at the same temperature as the surface to which they are attached,

d) The heat conduction from the wall in contact with the adsorbent will be evaluated through an equivalent convection heat transfer coefficient (relating the heat transfer to the sorbent from the metal surface to its temperature difference) with different values for the adsorbent close to the water channel and for the adsorbent in between the fins,

e) The equivalent convection heat transfer coefficient is uniform over the surface,

f) The overall heat transfer coefficient is uniform along the heat exchanger.

3.2 Overall thermal conductance estimation

The design of adsorber bed heat exchanger strongly affects the performance of adsorption chiller. Increasing the overall heat transfer coefficient (U) and heat transfer area (A) increase the overall heat transfer conductance (UA) and hence the chiller performance. Fig. 4(a) shows the control volume of a typical element from the adsorbent bed. It includes two half fins attached to the bed wall at the base which is in contact with the secondary fluid at temperature (T_w). The fins are in contact with silica gel from both sides and water vapor above it at (T_{ads}). Fig. 4(b) shows schematically the equivalent heat transfer thermal resistance of the adsorbent bed. During the heat transfer from/to the secondary fluid to/from the adsorbent bed surface in desorption/adsorption mode, there are four heat transfer resistances namely; (i) convection thermal resistance from the secondary fluid stream (water) to the internal tube wall ($1/h_w A_{w,i}$); (ii) conduction resistance through the plate wall ($e_{met}/k_{met}.A_{plate,i}$) and (iii) convection resistances for the unfinned surface as well as along the fins, which act in parallel. Therefore, the total thermal resistance from the water to the adsorbent in one control volume (i) can be expressed by:

$$R_{tot} = \frac{1}{h_w A_{w,i}} + \frac{e_{met}}{k_{met} A_{plate,i}} + \frac{1}{h_{eq,1} A_{unfin,i} + h_{eq,2} \eta_f A_{fin,i}} \quad (1)$$

where, the heat transfer area A for water side, finned and unfinned surfaces can be defined by $A_{w,i} = A_{plate,i} = p_f D$, $A_{fin,i} = 2(p\text{-}t)D/2$ and $A_{unfin,i} = (p_f\text{-}t_f) D$ respectively. The fin efficiency η_f may be defined as:

$$\eta_f = \frac{\tanh(mL_f)}{mL_f} \quad (2)$$

where

$$m = \sqrt{\frac{p_f h_{eq.2}}{A_{c,f} k_{met}}} = \sqrt{\frac{2Dh_{eq.2}}{t_f D k_{met}}} = \sqrt{\frac{4k_{ads}}{k_{met} t_f (p_f - t_f)}} \quad (3)$$

$$L_f = \frac{(p - t)}{2} \quad (4)$$

Hence,

$$mL_f = \frac{1}{2}\sqrt{\frac{4k_{ads}}{k_{met}}}\sqrt{\frac{1}{\frac{p_f}{p}(\frac{t_f}{p})^{-1} - 1}}(\frac{t_f}{p})^{-1}(1 - \frac{t}{p}) \quad (5)$$

The equivalent convection heat transfer coefficients for the finned ($h_{eq,2}$) and unfinned ($h_{eq,1}$) wall surfaces to the adsorbent can be estimated as the ratio of the adsorbent thermal conductivity to the corresponding distance between the adsorbent at mean temperature T_{ads} and the outer wall surface temperature $T_{s,o}$ as:

$$h_{eq,1} = \frac{k_{ads}}{(\frac{p - t}{4})} = \frac{4k_{ads}}{(p - t)} \tag{6}$$

$$h_{eq,2} = \frac{k_{ads}}{(\frac{p_f - t_f}{4})} = \frac{2k_{ads}}{(p_f - t_f)} \tag{7}$$

The convective heat transfer coefficient on the water side h_w can be estimated by assuming the hypothesis of fully developed laminar flow and a channel geometry similar to infinite parallel plates. Therefore, the convective heat transfer coefficient on the water side h_w becomes a function of the Nusselt number (N_u):

$$h_w = k_w \frac{N_u}{D_h} \tag{8}$$

where, the N_u value corresponding to the channel geometry and have a value of 7.54 [31] assuming the hypothesis of laminar flow with uniform wall temperature in a narrow rectangular channel. The hydraulic diameter (D_h) of the water channel equal to D = 2(t-2e_{met}).

The total heat transfer from the water to the adsorbent in one control volume i can be expressed as:

$$\dot{Q}_i = \frac{T_w - T_{ads}}{\frac{1}{A_{w,i}}\left[\frac{1}{k_w \frac{7.54}{2(t-2e_{met})}} + \frac{e_{met}}{k_{met}} + \frac{1}{\frac{4k_{ads}}{(p-t)}\left(\frac{p_f - t_f}{4}\right) + \frac{2k_{ads}}{(p_f - t_f)}\eta_f\left(\frac{p-t}{p_f}\right)}\right]} \qquad (9)$$

Therefore, the overall thermal conductance of the adsorbent bed heat exchanger $UA_{total,HE}$ can be estimated as

$$UA_{total,HE} = \frac{1}{\frac{1}{\left(k_w \frac{7.54}{2p\left(\frac{t}{p} - 2\frac{e_{met}}{p}\right)}\right)} + \frac{e_{met}}{k_{met}} + \frac{p\left(1-\frac{t}{p}\right)}{4k_{ads}\left(1-\frac{t_f}{p_f} + \frac{\eta_f}{2}\left[\frac{p^2\left(1-\frac{t}{p}\right)^2}{p_f^2\left(1-\frac{t_f}{p_f}\right)}\right]\right)}} A_{w,t} \qquad (10)$$

where $A_{w,t}$ is the total heat transfer area of the water side and can be written by:

$$A_{w,t} = \frac{W}{p} 2DH = \frac{2}{p} V_{HE} \qquad (11)$$

where V_{HE} =WDH is the overall volume of the heat exchanger. The mass of adsorbent which fits inside the bed heat exchanger can be evaluated by the empty volume inside the heat exchanger and the average density of the adsorbent grains (ρ_{ads}), resulting:

$$m_{ads,HE} = \rho_{ads} V_{HE} \left[\left(1 - \frac{t}{p} \right) \left(1 - \frac{t_f}{p_f} \right) \right] \tag{12}$$

Finally, the 'specific thermal conductance' of the adsorbent bed can be defined as the overall thermal conductance of the adsorbent bed heat exchanger ($UA_{tot,HE}$) divided by the overall volume of the heat exchanger:

$$\frac{UA_{total,HE}}{V_{HE}} = \frac{1}{\dfrac{1}{\left(k_w \dfrac{7.54}{2p(\frac{t}{p} - 2\frac{e_{met}}{p})} \right)} + \dfrac{e_{met}}{k_{met}} + \dfrac{p(1-\frac{t}{p})}{4k_{ads}\left(1 - \dfrac{t_f}{p_f} + \dfrac{\eta_f}{2}\left[\dfrac{p^2(1-\frac{t}{p})^2}{p_f^2(1-\frac{t_f}{p_f})} \right] \right)}} \frac{2}{p} \tag{13}$$

As it can be observed, the specific thermal conductance of the adsorbent bed is a complex analytical expression which only depends on the following geometrical and thermal parameters:

$$\frac{UA_{total,HE}}{V_{HE}} = f(k_w, k_{ads}, k_{met}, p, \frac{t}{p}, \frac{p_f}{p}, \frac{t_f}{p_f}, \frac{e_{met}}{p}) \tag{14}$$

When the cannel pitch p in between the flat tube has been taken as the proper length to make non-dimensional the rest of geometrical parameters.

3.3 Performance estimation

The performance of the actual adsorption system has been quantified by the maximum practical specific cooling capacity ($SCC_{m,p}$) and the maximum practical coefficient of performance ($COP_{m,p}$) that could be achieved in practical operation of the system. This two conditions cannot be reached at the same time. In general, maximum COP in practice is obtained at very long cycle periods, while maximum cooling capacity is obtained at much shorter periods.

3.3.1 Maximum coefficient of performance

The maximum practical COP for an adsorption system can be approached by:

$$COP_{m,p} = \frac{Q_{chill,m,p}}{Q_{heat}} = \frac{m_{ads,HE}\Delta w \Delta h_{fg}}{m_{ads,HE}\Delta w \Delta h_{des} + (m_{adsHE}cp_{ads,0} + m_{w,tot}cp_w + m_{met,tot}cp_{met})\Delta T_{bed}} \tag{15}$$

The term in the numerator of Eq. (15) represents the latent heat of vaporization of the refrigerant assuming that the adsorbent goes through the maximum possible uptake change (Δw). In the denominator, the first term refers to the heat input required for the desorption of the same amount of adsorbate/refrigerant, while the second term represents the sensible heat required to heat the adsorbent, the heat transfer fluid and the metallic parts of the heat exchanger along the heating phase, for the maximum bed temperature change, ΔT_b.

Dividing Eq. (15) by the term ($m_{ads,HE}\Delta w\Delta h_{des}$), the following equation can be got

$$COP_{m,p} = \frac{\Delta h_{fg} / \Delta h_{des}}{1 + \overline{c}p_{bed}(\frac{\Delta T_{bed}}{\Delta w \Delta h_{des}})} \quad (16)$$

where, the equivalent heat capacity of the bed per adsorbent mass ($\overline{CP}_{bed}$) is given by

$$\overline{c}p_{bed} = \left[cp_{ads,0} + (\frac{m_{w,tot}}{m_{ads,HE}})cp_w + (\frac{m_{met,tot}}{m_{ads,HE}})cp_{met} \right] \quad (17)$$

The maximum theoretical COP_{max} of an adsorption system is defined as the ratio between the enthalpy of vaporization and the enthalpy of desorption [32]:

$$COP_{max} = \frac{\Delta h_{fg}}{\Delta h_{des}} \quad (18)$$

Hence, Eq. (16) can be written as:

$$COP_{m,p} = \frac{COP_{max}}{1 + \bar{c}p_{bed}\left(\frac{\Delta T_{bed}}{\Delta w \Delta h_{des}}\right)} \tag{19}$$

The $COP_{m,p}$ of Eq. (19) takes into account the heating/cooling losses of all masses present in the bed (i.e. metal, adsorbent and heat transfer fluid masses). The actual values of COP will be lower than the $COP_{m,p}$ because of other irreversibilities such as pressure losses between the bed and the condenser/evaporator and heat losses.

In practical operation of the system, the maximum ($T_{bed,M}$) and minimum ($T_{bed,m}$) bed temperatures do not achieve the temperatures of the external heating ($T_{hw,in}$) and cooling ($T_{cw,in}$) water sources. Therefore, the maximum temperature variation in the bed (ΔT_{bed}) could be corrected by a correction factor φ.

$$\Delta T_{bed} = T_{bed,M} - T_{bed,m} \cong \varphi(T_{hw,in} - T_{cw,in}) \tag{20}$$

Based on the operating conditions mentioned in Table 2, the simulation results showed that the factor φ has been found between 0.90-0.95.

The maximum uptake variation in the bed (Δw) corresponds to the difference between maximum (w_{max}) and minimum (w_{min}) uptakes, defined by

$$\Delta w = w_{max} - w_{min} \tag{21}$$

The equilibrium uptake in the bed (w_{eq}) depending on the temperatures and pressures can be estimated by [33]:

$$\ln(p) = a_0 + a_1 w_{eq} + a_2 w_{eq}^2 + a_3 w_{eq}^3 + \frac{b_0 + b_1 w_{eq} + b_2 w_{eq}^2 + b_3 w_{eq}^3}{T} \tag{22}$$

where, the numerical values of the coefficients a and b (i = 0, 1, 2, 3) for silica-gel (Sorbsil A) are given by Restuccia [34].

Hence, the maximum and minimum uptakes can be defined as:

$$w_{max} = w_{eq}(P_{evap}, T_{bm}) \cong w_{eq}(P_{evap}, T_{cw,in}) \tag{23}$$

$$w_{min} = w_{eq}(P_{cond}, T_{bM}) \cong w_{eq}(P_{cond}, T_{hw,in}) \tag{24}$$

where, P_{evap} and P_{cond} are the evaporator and condenser pressures, respectively.

$$P_{evap} = P_{sat}(T_{evap}) \cong P_{sat}(T_{chw,in}) \tag{25}$$

$$P_{cond} = P_{sat}(T_{cond}) \cong P_{sat}(T_{cw,in}) \tag{26}$$

where, $T_{chw,in}$ is the chilled water inlet temperature and $T_{cw,in}$ is the condenser cooling water inlet temperature.

The desorption heat (Δh_{des}) at a specified uptake (w_{min}) can be estimated by the following equation [33]:

$$\Delta h_{des}(w_{min}) = -(b_0 + b_1 w_{min} + b_2 w_{min}^2 + b_3 w_{min}^3 + \frac{R}{M_w} \qquad (27)$$

where, the numerical values of the coefficients b (i = 0, 1, 2, 3) for silica-gel (Sorbsil A) are given by Restuccia [34].

The specific heat of vaporization of the water (Δh_{fg}) at a specified temperature (T) can be estimated by [35]:

$$\Delta h_{fg}(T) = 3159.2\times10^3 - 2406.7T \qquad (28)$$

The specific heat of vaporization of the water is estimated at the following hypothetical temperature conditions:

$$\Delta h_{fg} = \Delta h_{fg}(T_{evap}) \cong \Delta h_{fg}(T_{chw,in}) \qquad (29)$$

3.3.2 Maximum practical specific cooling capacity

Assuming the overall heat transfer coefficient is constant along the heating period, the total heat given by the heating water to the bed in order to desorb the refrigerant along the heating period can be estimated as:

$$Q_{heat} = UA_{total,HE}(T_{hw,in} - \tilde{T}_{bed})\frac{\tau}{2} \qquad (30)$$

where, $\breve{T}_b$ is the mean temperature of the bed which is defined as:

$$\tilde{T}_{bed} = \frac{\int_0^{\tau/2} T_{bed} dt}{\tau / 2} \tag{31}$$

Where, the mean temperature of the bed $\tilde{T}_{bed}$ depends on the maximum and minimum temperatures of the bed, and it should be more close to $T_{bed,M}$ since the bed is in heating mode. However, in order to simplify the calculus it has been assumed that $\breve{T}$ is the arithmetic mean between the heating and cooling water temperatures.

$$\tilde{T}_{bed} = \frac{T_{bed,M} + T_{bed,m}}{2} \cong \frac{T_{hw,in} + T_{cw,in}}{2} \tag{32}$$

Assuming that the overall heat transfer coefficient is constant along the heating period, Eq. (30) can be written as

$$Q_{heat} \cong UA_{total,HE} \left(\frac{T_{hw,in} - T_{cw,in}}{2}\right) \frac{\tau}{2} \tag{33}$$

The maximum practical COP taking into account the heating/cooling losses can be expressed as:

$$COP_{m,p} = \frac{m_{ads} \Delta w \Delta h_{fg}}{Q_{heat}} \tag{34}$$

Assuming that at the maximum cooling the amount of desorbed water is closed to the one that can be desorbed with a longer time, i.e. at maximum practical COP, and tacking in to account that the same amount of water desorbed is fully condensed and then evaporated, the maximum cooling capacity of the system can be evaluated as:

$$Q_{chill,mp} = \frac{m_{ads}\Delta w \Delta h_{fg}}{\tau} = \frac{1}{2} UA_{total,HE} \left(\frac{T_{hw,in} - T_{cw,in}}{2}\right) COP_{m,p} \quad (35)$$

The above equation relates the maximum cooling capacity with the maximum practical $COP_{m,p}$.

Finally, the maximum practical cooling capacity per volume of heat exchanger ($SCC_{m,p}$), becomes

$$SCC_{m,p} = \left.\frac{Q_{chill,mp}}{V_{HE}}\right|_{m,p} \cong \frac{1}{2} \frac{UA_{total,HE}}{V_{HE}} \left(\frac{T_{hw,in} - T_{cw,in}}{2}\right) COP_{m,p} \quad (36)$$

Considering Eq.14, Eq.16 and Eq.36 it can be concluded that $SCC_{m,p}$ depends on the material properties, bed design and operating parameters:

$$SCC_{m,p} = f\left(\frac{\Delta h_{fg}}{\Delta h_{des}}, \Delta h_{des}, c\overline{p}_{bed}, T_{hw,in}, T_{cw,in}, T_{chw,in}, k_w, k_{ads}, k_{met,} p, \frac{t}{p}, \frac{p_f}{p}, \frac{t_f}{p}, \frac{e_{met}}{p}\right) \quad (37)$$

4. Results and discussion

The effect of design and thermal parameters on the system performance has been investigated based on the mathematical model developed in the previous sections. This was done with the aim of finding the optimal bed design parameters which will allow the system to reach the best heat transfer performance. Several parametric studies have been carried out with reference to the base-case bed. The standard operating conditions are shown in Table 2 [22, 23], whereas the base case thermal parameters are listed in Table 3.

The water thermal conductivity has been estimated for a water temperature of 61.5 ºC, since it corresponds to the average of nominal water temperature mentioned in Table 2.

In order to study the effect of different design and thermal parameters, the parameters shown in Table 4 are changed accordingly. Unless stated otherwise, the base-case parameter values adopted in the parametric studies are the ones reported on Table 1 - 3.

4.1 Sorbent material, main design and operating parameters

In this section, firstly the effect of different working pair on the $COP_{m,p}$ and $SCC_{m,p}$ is discussed and then the effect of water/adsorbent bed mass ratio and operating temperatures will be presented for the reference working pair silica-gel (sorbil A).

Fig. 5 presents a comparison between the effects of different working pairs on the system performance described by the $COP_{m,p}$ and $SCC_{m,p}$ as a function of the desorption heat. Table 5 presents the adsorption properties of the different working pairs considered.

As it can be observed, the desorption heat of the working pair has a significant influence on the maximum performance of the system. The maximum performance is higher for working pairs having low desorption heat, this is due to the fact that less heat input is required for the bed to desorb and adsorb the refrigerant, as well as lower heat losses associated. Changing the base-case working pair from Sorbsil A/water (Δh_{des}=3115.9 KJkg-1) to SWS-1L/water (Δh_{des}=2610.4 kJkg^{-1}) could increase both $COP_{m,p}$ and $SCC_{m,p}$ by approximately 38%. Therefore, it is convenient to choose a working pair with low desorption heat and low adsorbent specific heat capacity in order to reduce the heat losses.

Figs. 6 shows the effect of water/adsorbent mass ratio and metal/adsorbent mass ratio on the system performance. Decreasing $m_{w,tot}/m_{ads,HE}$ ratios lead to increase both the $COP_{m,p}$ and $SCC_{m,p,}$ as shown in Fig. 6(a). Lower amount of water in the heat exchanger requires less heat input for sensible heating the bed and hence increases the performance of the system. Therefore, the water/adsorbent mass ratio should be kept as low as possible in order to avoid heat losses. This can be accomplished by reducing the internal volume of the water channels and headers.

Decreasing $m_{met,tot}/m_{ads,HE}$ ratios result in an increase of both $COP_{m,p}$ and $SCC_{m,p,}$ as shown in Fig. 6 (b). A smaller amount of metal requires less heat input for heating the inert masses of the bed. On the other hand, the performance of the system could be significantly enhanced by considering metal components and adsorbents for the bed that have low specific heat capacities, in order to avoid heat losses and other energy losses associated to the alternate heating and cooling, in addition to high thermal conductivity.

Finally, the effect of operating temperatures on the $COP_{m,p}$ and $SCC_{m,p}$ is shown in **Fig. 7 (a-c).** The $COP_{m,p}$ tends to increase when decreasing the $T_{hw,in}$ and $T_{cw,in}$, and increases when increasing the $T_{chw,in}$. On the other hand, the $SCC_{m,p}$ increases with increasing in $T_{hw,in}$ and $T_{chw,in}$ and decreasing $T_{cw,in}$.

As shown in Fig. 7 (a), increasing $T_{hw,in}$ from 70 to 120 ºC decreases the $COP_{m,p}$ by 19.7 % from 0.57 to 0.46 and increases the $SCC_{m,p}$ by 88.7 % from 836.5 to 1579 kWm^{-3}. This is because the cooling capacity and the heat losses increase both with higher driving source temperature. Therefore, an optimum design should balance the increased cooling capacity due to higher heating water temperatures against the poorer $COP_{m,p}$ resulting from larger heat inputs. Both $SCC_{m,p}$ and $COP_{m,p}$ increase with lower cooling water inlet temperature, due to the increase of the adsorption rate as shown in Fig. 7(b). However, the $SCC_{m,p}$ is more sensitive to $T_{cw,in}$ variations than $COP_{m,p}$. Increasing $T_{cw,in}$ from 20 to 40 ºC, decreases the $COP_{m,p}$ by 21.2 % and $SCC_{m,p}$ by 43.70 %. Decreasing the chilled water temperature results in less cooling produced, and therefore lower adsorption rates. Decreasing $T_{chw,in}$ from 20 to 5 ºC, both $COP_{m,p}$ and $SCC_{m,p}$ decreased by 28.9%, Fig. 7(c).

4.2 Bed geometrical parameters

In this section, the effect of bed geometrical parameters such as p, t/p, p_f/p, t_f/p, e_{met}/p, k_{ads}, k_{met} and k_w on the specific thermal conductance of the bed and $SCC_{m,p}$ will be presented.

Fig. 8 shows that both the specific thermal conductance and $SCC_{m,p}$ dramatically decrease with increasing channel pitch p. This is because the total thermal resistance increases with channel pitch, since the conductive path length increases. Reducing the distance between the water channels enhances the heat transfer performance since the conduction through the adsorbent is poor. For closely spaced channels the heat will be quickly transferred, and consequently the conduction through the adsorbent will improve. However, it should be taken into consideration that the adsorbent granules must still be able to fit in between the channels.

Significant performance improvements could be achieved with channel pitches smaller than 0.004 m. Reducing the channel pitch from its design value (p=0.0067 m) to a minimum permissible value (e.g. p=0.004 m) increases the specific thermal conductance and $SCC_{m,p}$ by approximately 2.5 times its original value. Therefore, the following parametric studies have been carried out for both the channel pitch design value (p=0.0067 m) and the reduced pitch value (p=0.004), in order to compare both performances.

Fig. 9 shows the effect of t/p variation on specific thermal conductance and $SCC_{m,p}$ for both the base-case bed (Fig. 9(a)) and the reduced pitch bed (Fig. 9(b)). The specific thermal conductance and $SCC_{m,p}$ decrease as the t/p ratio (t/p) increases for both cases, however, this variation is smoother than the previous one shown in Fig. 8.

Decreasing the flat tube thickness (t) results in an increase of the water velocity in the channels and therefore enhances the convection heat transfer coefficient at the water side, so that the overall heat transfer performance of the bed increases. Significant performance improvements could be achieved for the reduced pitch of 4 mm. For the base-case bed, the maximum practical specific cooling capacity increases from 632 to 1481 kWm^{-3} for a t/p from 0.668 reduced to 0.16. For the reduced pitch, the maximum practical specific cooling capacity increases from 1772 to 4156 kWm^{-3} for a t/p from 0.668 to 0.16 respectively, with an improvement of more than 2.3 times the original value.

In Fig. 10, the effect of fin thickness is analyzed. As it can be seen, both the specific thermal conductance and $SCC_{m,p}$ increase with the t_f/p increase but only very slightly. This can be explained by the fact that increasing the fin thickness enhances the heat conduction along the fins, thus improving the heat transfer to the adsorbent. However the increase is moderate because the high conductivity of aluminum. The maximum practical specific cooling capacity increases from 3499 to 3966 kWm^{-3} for a t_f/p from 0.005 to 0.0278, about 13.3 % of improvement of the base-case bed. Anyhow, increasing the fin thickness would increase the ratio of metal to sorbent mass ratio which clearly would negatively affect the performance. The combined effect of these parameters should be investigated before recommending any change in regard to the design value.

Fig. 11 shows that, decreasing the fin pitch/channel pitch ratio (p_f/p) enhances significantly both specific thermal conductance and $SCC_{m,p}$. This can be explained by the fact that decreasing fin pitch results in increasing the number of fins, which will increase the heat transfer performance of the bed and hence the maximum practical specific cooling capacity. For the base-case bed, the $SCC_{m,p}$ increases from 400 to 3000 kWm^{-3} for a t_f/p from 0.1 to 0.555 respectively. However, the performance could be significant enhanced with the reduced pitch. In this case, the maximum practical specific cooling capacity increases from 1100 to 7000 kWm^{-3} for a t_f/p from 0.1 to 0.555. Thus, a better heat performance of the bed could be achieved by means of reducing the distance between the fins. In any case one must take into account that the sorbent grain must still be able to fit in between the fins.

Fig. 12 shows that, the specific thermal conductance and $SCC_{m,p}$ slightly increase with increasing e_{met}/p ratios. Increasing the water channel wall thickness enhances the water velocity in the channel for a fixed water mass flow rate, and hence the convection heat transfer coefficient from the water to the adsorbent. For the base-case bed, the $SCC_{m,p}$ increases from 1150 to 1391 kWm^{-3} for a e_{met}/p from 0.0298 to 0.0936 respectively. The enhancement with a reduced pitch is much higher, where the maximum practical specific cooling capacity increases from 3227 to 3904 kWm^{-3} for e_{met}/p from 0.0298 to 0.0936 respectively. However, the increase in velocity also leads to an increase of the pressure drop and hence the pumping work. Therefore, an optimization considering both effects is necessary.

Fig. 13 shows a comparison of the combined effect of t/p and p_f/p (which are the most important parameters affecting the specific thermal conductance of the bed as it has been shown) versus the specific thermal conductance and $SCC_{m,p}$ for the two considered pitch cases. Decreasing t/p and p_f/p improve the specific thermal conductance of the bed. However there is a significant increase in specific thermal conductance for t/p less than 0.16 and p_f/p less than 0.10. High performance improvements could be achieved with a reduced pitch of 0.004 m. In this case, by decreasing the t/p and p_f/p from 0.25 and 0.22 to nearly 0.16 and 0.10 may increase the specific thermal conductance from 463 to 1727 kWm^{-3}. This is a very significant improvement by almost three times the original value.

4.3 Thermal conductivity

The effect of thermal parameters such as the adsorbent (k_{ads}) and metal thermal conductivities (k_{met}) and the heat transfer fluid thermal conductivity (k_w) on the specific thermal conductance and the $SCC_{m,p}$ are discussed in this section.

Two basic assumptions have been made in this analysis. The major assumption is about the effective adsorbent thermal conductivity of the bed, which is very difficult to estimate and depends on many factors such as gas pressure, porosity, etc. According to the literature [38], the effective thermal conductivity of a granular adsorbent bed (including adsorbent grains plus interparticle voids) varies from 0.06 W $m^{-1}K^{-1}$ in case of very loose grains to 0.2 W $m^{-1}K^{-1}$ in case of compacted grains. Taking into account the above, the mean value within this range has been assumed for the effective adsorbent thermal conductivity of the bed, e.g. 0.13 W $m^{-1}K^{-1}$. The second assumption concerns the value of the water thermal conductivity. This parameter has been estimated for a water temperature of 61.5 ºC, since it corresponds to the average temperature between heating the bed at 90 ºC and cooling the bed at 33 ºC.

From Fig. 14 it can be observed that, the adsorbent thermal conductivity (k_{ads}) is a very sensitive parameter which positively affects the heat transfer performance. As expected, higher k_{ads} results in considerable better performance. The specific thermal conductance increases from 157 to 211.5 $kWm^{-3}K^{-1}$ by increasing the k_{ads} from its design value 0.13 $Wm^{-1}K^{-1}$ for the granular adsorbent bed under consideration to 0.20 $Wm^{-1}K^{-1}$. It has been found that an adsorbent thermal conductivity exceeding 0.15 $Wm^{-1}K^{-1}$ is desirable.

Obviously, he conduction through the adsorbent constitutes the major portion of the total thermal resistance in the bed. Therefore, the design efforts should be focused on reducing the thermal resistance through the adsorbents [27]. Mixing the adsorbent with metallic foam increases the adsorbent thermal conductivity and hence improve the heat transfer performance [25]. Coating the adsorbent bed metal with the adsorbent can be eliminate the contact thermal resistance [39]. Decrease the intergranular porosity of the adsorbent by mixing together grains of various sizes can also be improve the equivalent thermal conductivity of the bed, since the vapor that surrounds the grains has low thermal conductivity [24].

Fig. 15 shows the effect of the metal thermal conductivity of the bed on the specific thermal conductance and the $SCC_{m,p}$. The results show that, k_{met} does not have a significant effect on the heat transfer performance. However, a metal thermal conductivity of at least 140 W $m^{-1}K^{-1}$ is desirable, exceeding this value does not yield significant benefits. Changing the material of the heat exchanger from aluminum (160 $Wm^{-1}K^{-1}$) to copper (400 $Wm^{-1}K^{-1}$) will not result in a performance enhancement, since its thermal capacitance it's much higher and heat losses of alternative heating and cooling will increase. On the other side, employing low conductivity materials like plastics could lead to an important loss of performance.

Finally, Fig. 16 shows the effect of heat transfer fluid thermal conductivity on the specific thermal conductance of the bed and the $SCC_{m,p}$, at different channel pitch values. Two different heat transfer fluids have been considered, pure water with thermal conductivity of 0.656 $Wm^{-1}K^{-1}$, which corresponds to the base-case study and the other one is a 30% ethylene glycol-water mixture with thermal conductivity of 0.5 $Wm^{-1}K^{-1}$ [36].

It can be observed that the fluid thermal conductivity does not have a significant effect on the system performance, only an small decrease of the specific thermal conductance of the bed, and hence on the temperature variation along the heat exchanger can be observed. It is clear that fluid-side convection heat transfer resistance has a very small contribution on the total thermal resistance in the bed. Nevertheless, the use of a brine could result in increased pressure losses in the channel. This would increase the pumping work, and therefore contribute negatively to the actual COP of the system.

5. Conclusions

Enhancing heat and mass transfer in the adsorbent bed significantly improves the overall efficiency and performance of the adsorption system. High performance, small size, and low weight are critical requirements for any bed heat exchanger used in automobile air conditioning applications. An analytical model has been developed to analyze the influence of adsorbent bed parameters on the overall thermal conductance of the bed as well as to assess the maximum performance that could be achieved with a properly designed and operated system. Results showed that reducing the channel pitch from the initial value to a minimum permissible value increases the specific thermal conductance and maximum practical specific cooling capacity by approximately 2.5 times its original value. Decreasing in the t/p and p_f/p ratios provide high heat transfer rate throughout the bed. The effect is most apparent for t/p less than approximately 0.21 and p_f/p less than approximately 0.13. On the other hand, increasing t_f/p and e_{met}/p ratios positively affects the specific thermal conductance of the bed.

From all thermal parameters that have been studied, it is found that adsorbent thermal conductivity is the most sensitive parameter to the system performance. Increasing the adsorbent thermal conductivity clearly results in better system performance. A metal thermal conductivity of at least 140 $Wm^{-1}K^{-1}$ is desirable, which is well reached by employing aluminum. With a reduced pitch p of 4 mm an still possible water flat tube thickness 0.8 mm, and similar fin pitch 0.8 mm, the $SCC_{m,p}$ with silica-gel (sorbsil A) at reference operation conditions could be 850 kW/m^3. What could lead to a potential cost effective technology. Still, the problem of placing the sorbent material in between the fins including a relatively high thermal conductivity, and still enough permeability to the vapor flow, must be solved adequately. On the way to more efficient and economic cooling systems, future research attention should be focused on improving the heat and mass transfer inside the adsorbent bed.

Acknowledgements

This work has been partially supported by the Thermally Operated Mobile Air Conditioning Systems (TOPMACS).

References

[1] K. Harby, R.G. Doaa, S.K. Nader, S.S Mohamed, Performance improvement of vapor compression cooling systems using evaporative condenser: An overview, Renew Sust. Energ Rev. 58 (2016) 347-360.

[2] H. Demir, M. Mobedi, and S. Ülkü, A review on adsorption heat pump: problems and solutions, Renewable and Sustainable Energy Reviews 12 (2008) 2381-2403.

[3] A.S. Alsaman, A. Askalany, K. Harby and M. Ahmed, A state of the art of hybrid adsorption desalination-cooling systems. Renewable and Sustainable Energy Reviews 2016;58:692-703.

[4] A. Sapienza, S. S antamaria, A. Frazzica, and A. Freni, Influence of the management strategy and operating conditions on the performance of an adsorption chiller, Energy 36 (2011) 5532-5538.

[5] M. Ghazy, A. Askalany, K. Harby, M Ahmed, Adsorption isotherms and kinetics of HFC-404A onto bituminous based granular activated carbon for storage and cooling applications. Applied Thermal Engineering 2016;105:639-645.

[6] M. Hamdy, A.A. Akalany, K. Harby, N. Koraa, An overview on adsorption cooling systems powered by waste heat from internal combustion engine, Renewable and Sustainable Energy Reviews 51 (2015) 1223-1234.

[7] M. Verde, L. Cortés, J.M. Corberán, A. Sapienza, S. Vasta, G. Restuccia, Modelling of an adsorption system driven by engine waste heat for truck cabin A/C. Performance estimation for a standard driving cycle, Appl Therm Eng 30 (2010) 1511-22.

[8] M. Ghazy, K. Harby, A.A. Akalany, B.B. Saha, Adsorption isotherms and kinetics of activated carbon/difluoroethane adsorption pair: theory and experiments, International Journal of Refrigeration, Accepted manuscript January 2016

[9] B. Choudhury, B.B. Saha, P.K. Chatterjee, J.P. Sarkar, An overview of developments in adsorption refrigeration systems towards a sustainable way of cooling, Appl. Energ 103 (2013) 554-567.

[10] D.C. Wang, Y.H. Li, D. Li, Y.Z. Xia, J.P. Zhang, A review on adsorption refrigeration technology and adsorption deterioration in physical adsorption systems, Renewable and Sustainable Energy Reviews 14 (2010) 344-353.

[11] A. Raymond, and S. Garimell, Annular-finned sorption bed heat exchanger design for adsorption heat pump optimization, In: Proc. of the International Sorption Heat Pump Conference ISHPC11 (2011) Padua, Italy.

[12] M. Linder, R. Mertz, E. Laurien, Experimental results of a compact thermally driven cooling system based on metal hydrides, International Journal of Hydrogen Energy 35 (2010) 7623-7632.

[13] M. Li, R.Z. Wang, Heat and mass transfer in a flat plate solar solid adsorption refrigeration ice maker, Renewable Energy 28 (2003) 613-622.

[14] R.Z. Wang, J.Y. Wu, Y.X. Xu, Y. Teng, W. Shi, Experiment on a continuous heat regenerative adsorption refrigerator using spiral plate heat exchanger as adsorbers, Applied Thermal Engineering 18 (1998) 13-23.

[15] B.B. Saha, S. Koyama, I.I. El-Sharkawy, K. Kuwahara, K.Kariya, K.C. Ng, Experiments for measuring adsorption characteristics of an activated carbon fiber/ethanol pair using a plate-fin heat exchanger, HVAC&R Research 12 (2006) 767-782.

[16] M.A. Lambertand, B.J. Jones, Automotive adsorption air conditioner powered by exhaust heat. Part 1: conceptual and embodiment design, Journal of Automobile Engineering 220 (2006) 959-972.

[17] Y.B. Gui, R.Z. Wang, W. Wang, J.Y. Wu, and Y.X. Xu, Performance modelling and testing on a heat-regenerative adsorptive reversible heat pump, Applied Thermal Engineering 22 (2002) 309-320.

[18] G. Restuccia, A. Freni, G. Maggio, A zeolite-coated bed for air conditioning adsorption systems: parametric study of heat and mass transfer by dynamic simulation, Applied Thermal Eng. 22 (2002) 619-630.

[19] L.Z. Zhang, Design and testing of an automobile waste heat adsorption cooling system, Applied Thermal Engineering 20 (2000) 103-114.

[20] R.E. Critoph, T.Z. Telto, and L.N. Davies, A prototype of a fast cycle adsorption refrigerator utilizing a novel carbon-aluminium laminate, In: Proc. of the Institution of Mechanical Engineers 214 (2000).

[21] P. Bou, Guilleminot, J.J. Pons Composite actifà structure feuilletée comprenant un agent actif sous forme de granules, Elf Aquitaine Patent, 9612762. (1996).

[22] M. Verde, K. Harby, Robert de Boer, José M. Corberán, Performance evaluation of a waste-heat driven adsorption system for automotive air-conditioning: Part I - Modeling and experimental validation, Energy, Accepted.

[23] M. Verde, K. Harby, Robert de Boer, José M. Corberán, Performance evaluation of a waste-heat driven adsorption system for automotive air-conditioning: Part II - Performance optimization under different real driving conditions, Energy, Accepted.

[24] J. J. Guilleminot, A. Choisier, J.B. Chalfen, S. Nicolas and J.L. Reymoney, Heat transfer intensification in fixed bed adsorbers, Heat Recovery Systems & CHP 13 (1993) 297-300.

[25] A. Rezk, R.K. Al-Dadah, S. Mahmoud, A. Elsayed, Effects of contact resistance and metal additives in finned-tube adsorbent beds on the performance of silica gel/water adsorption chiller, Applied thermal engineering 53 (2013) 278-284.

[26] N. Hamid, D. Iman, Numerical simulation of heat and mass transfer in adsorbent beds with annular fins, International Journal of Refrigeration 35 (2012) 581-593.

[27] N.H. Hamid Talebian, M. Mahdavikhah, Bed geometrical specifications effects on the performance of silica/water adsorption chillers, International Journal of Refrigeration 35 (2012) 2261-2274.

[28] A.R. Rezk, and R.K. Al-Dadah, Physical and operating conditions effects on silica gel/water adsorption chiller performance, Applied Energy 89 (2012) 142-149.

[29] M.Z Khan, K.C. Alam, B.B. Saha, Y. Hamamoto, A. Akisawa, and T. Kashiwagi, Parametric study of a two-stage adsorption chiller using re-heat-The effect of overall thermal conductance and adsorbent mass on system performance. International Journal of Thermal Sciences 45 (2006) 511-519.

[30] European project TOPMACS-Thermally Operated Mobile Air-Conditioning Systems, funded by the European Commission under the 6th European Community framework program (Contract Ref. TST4-CT-2005-012471). Retrieved from: http://ec.europa.eu/research/transport/projects/items/topmacs_en.htm

[31] F.P. Incropera, Fundamentals of Heat and Mass Transfer, 3rd Edition, Wiley, New York (1990) pp. 501.

[32] V.E. Sharonov, Y. Aristov, Chemical and adsorption heat pumps: Comments on the second law efficiency, Chemical Eng. Journal 136 (2008) 419-424.

[33] G. Cacciola, and G. Restuccia, Reversible adsorption heat pump: a thermodynamic model, International Journal of Refrigeration 18 (1995) 100 -106.

[34] G. Restuccia, Y. Aristov, G. Maggio, G. Cacciola, and M.M. Tokarev, Performance of sorption systems using selective water sorbents, In: Proc. of the International Sorption Heat Pump Conference-ISHPC99, Munich, Germany, (1999) 219-223.

[35] Rohsenow, W.M, Hartnett and Ganic, E.N. Handbook of heat transfer fundamentals, 2nd Edition, McGraw-Hill, (1985) New York.

[36] A. Melinder, Thermo-physical Properties of Liquid Secondary Refrigerants, IIR-International Institute of Refrigeration (1997).

[37] A.F. Mills, Heat Transfer. 2nd Edition, Prentice Hall, Upper Saddle River (1999).

[38] A. Freni, Personal communication, Istituto di Tecnologie Avanzate per l´Energia 'Nicola Giordano' CNR-ITAE, Messina, (2013) Italy.

[39] K.S. Chang, M.T. Chen, T.W. Chung, Effects of the thickness and particle size of silica gel on the heat and mass transfer performance of a silica gel-coated bed for air-conditioning adsorption systems, Applied Thermal Engineering 25 (2005) 2330-2340.

Figures

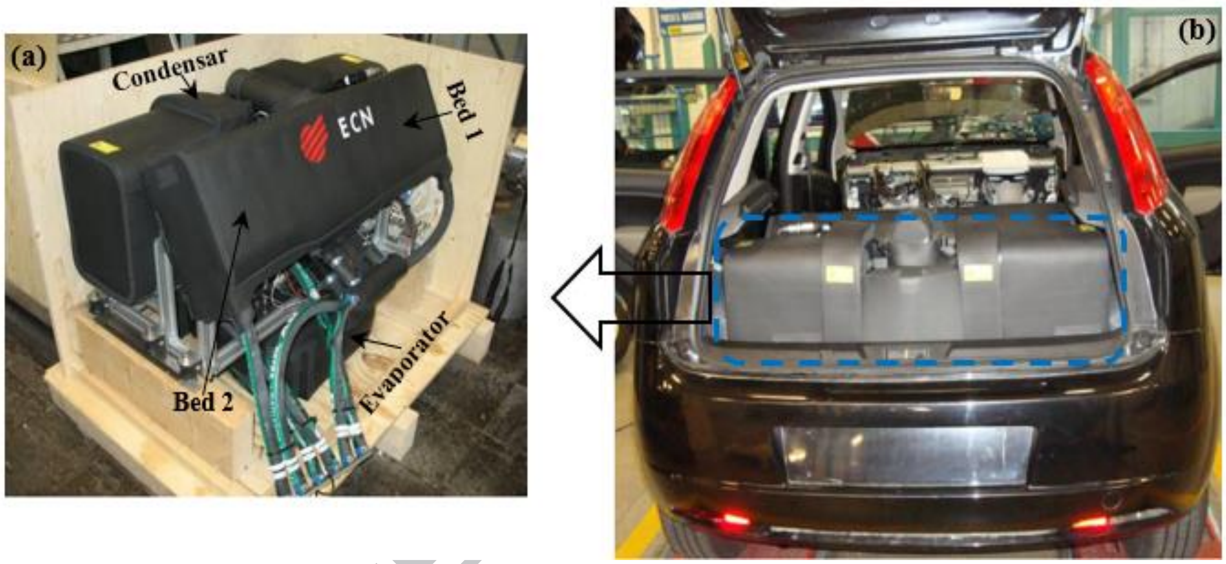

Fig. 1. Pictures of the onboard adsorption chiller: (a) in the laboratory and (b) installed in the vehicle

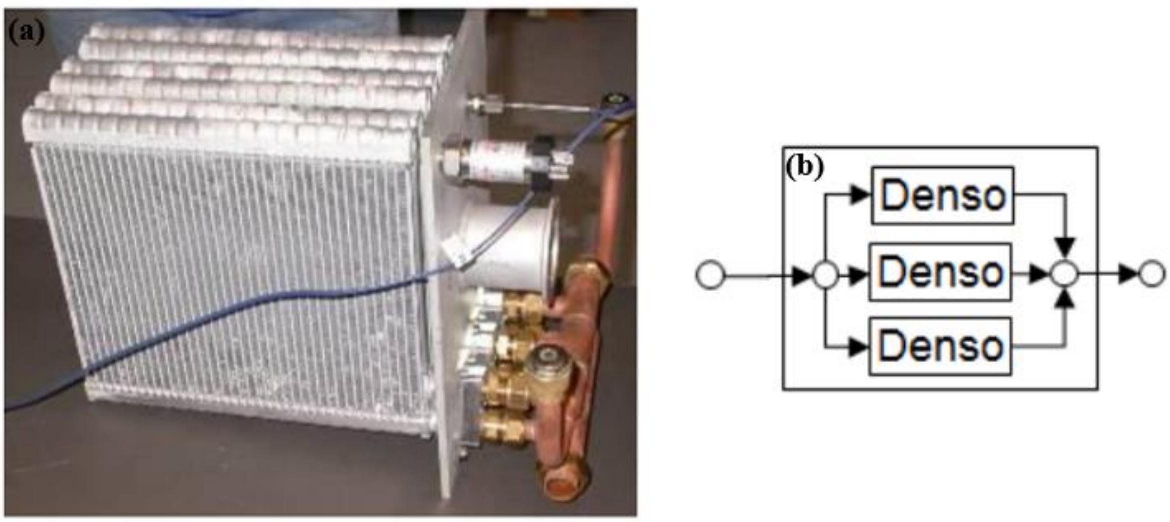

Fig. 2. Schematic diagram of a (a) single bed comprised of three heat exchangers and inlet/outlet header. (b) Bed water flow arrangement scheme.

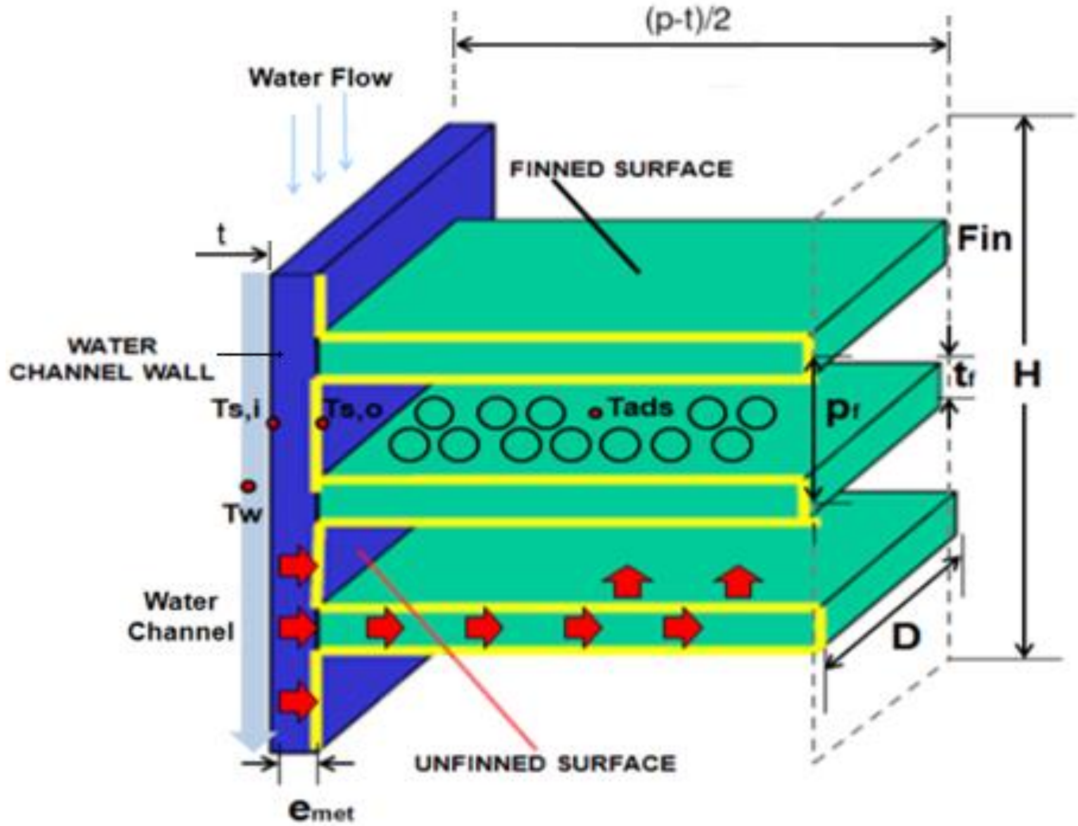

Fig. 3. Schematic diagram of the modelled adsorbent bed

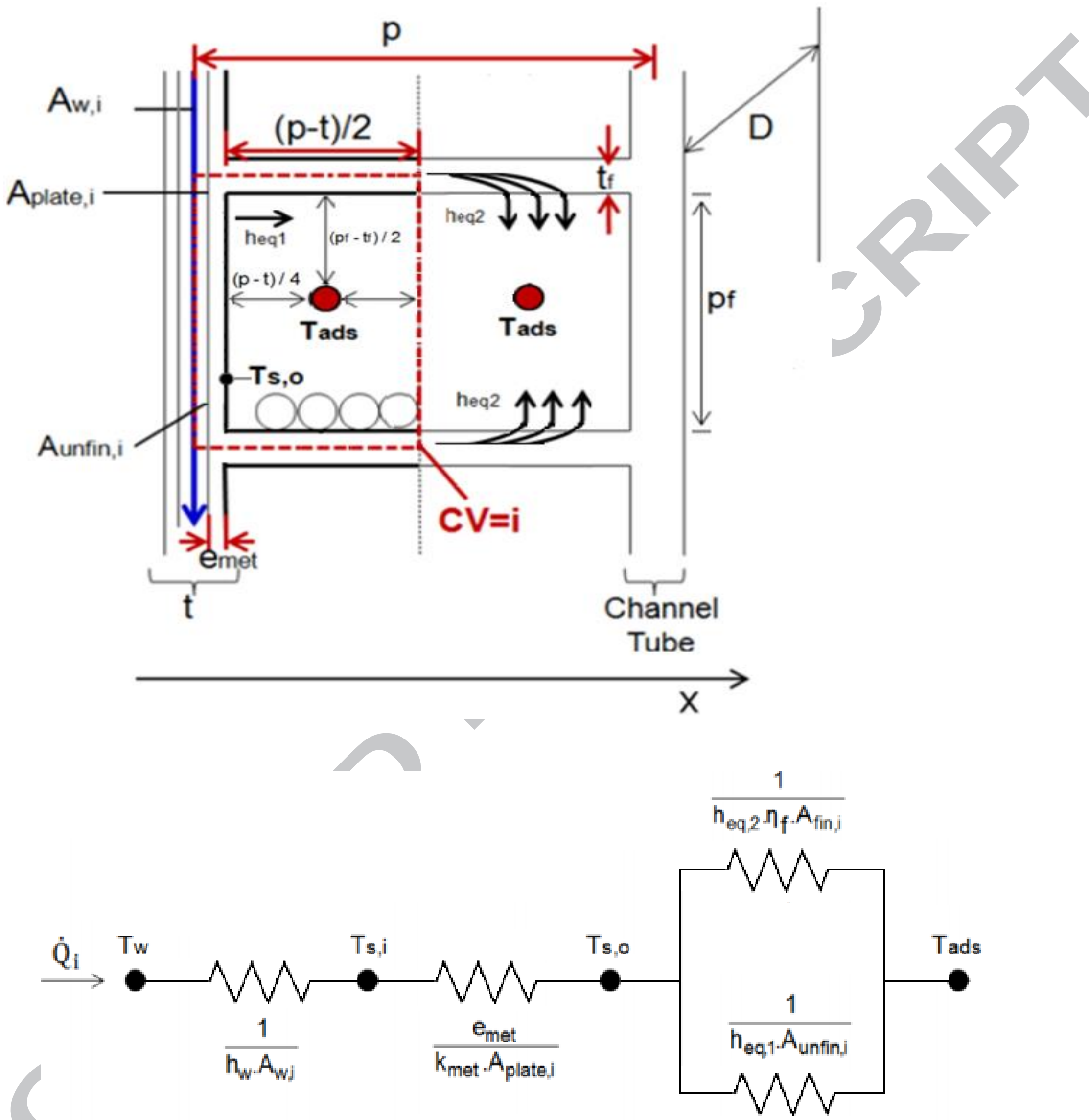

Fig. 4. Schematic diagram of the a) heat transfer through the adsorbent bed in one control volume and b) equivalent heat transfer thermal resistance

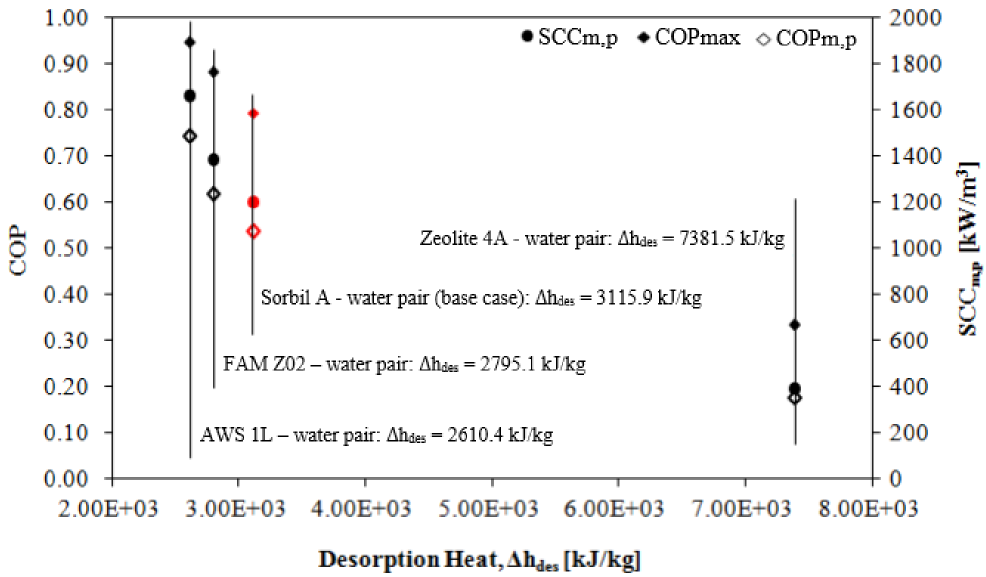

Fig. 5. Effect of different working pairs on the maximum theoretical and maximum practical COP as well as $SCC_{m,p}$

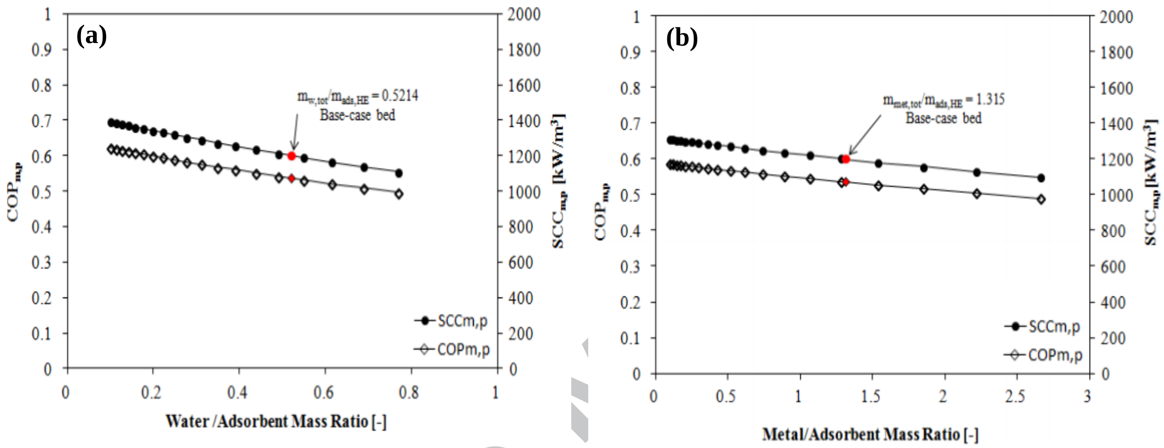

Fig. 6. Effect of a) water/adsorbent mass ratio and b) metal/adsorbent mass ratio on the $COP_{m,p}$ and $SCC_{m,p}$

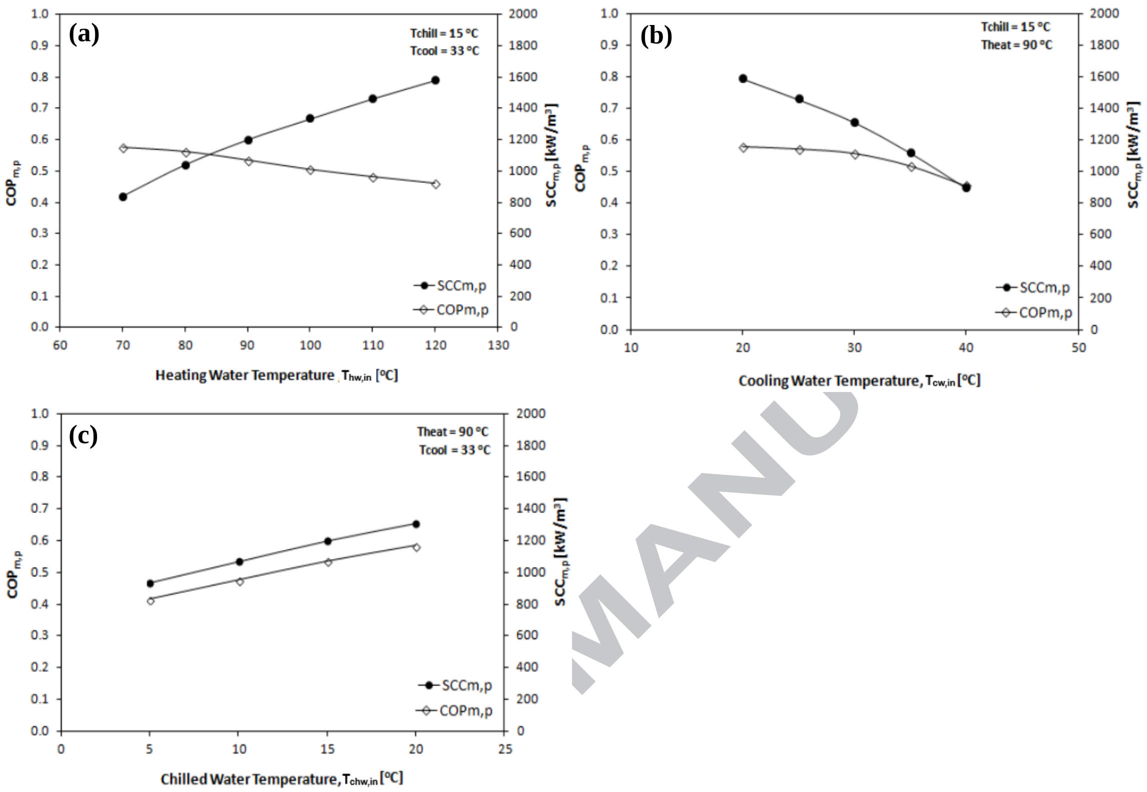

Fig. 7. Effect of a) hot b) cooling and c) chilled water inlet temperatures on the $COP_{m,p}$ and $SCC_{m,p}$

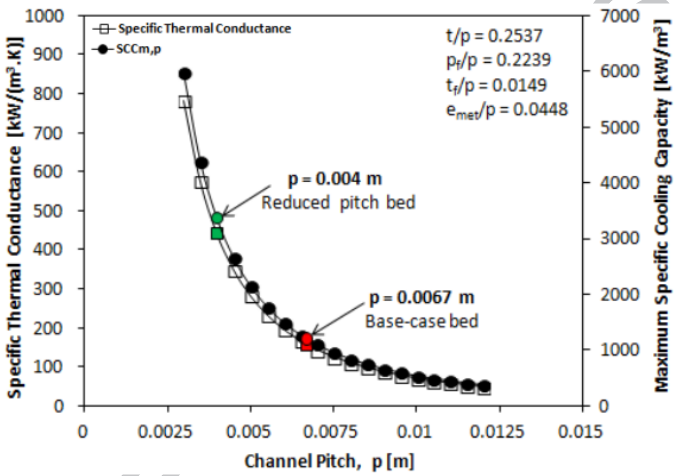

Fig. 8. Effect of channel pitch p on specific thermal conductance of the bed and $SCC_{m,p}$

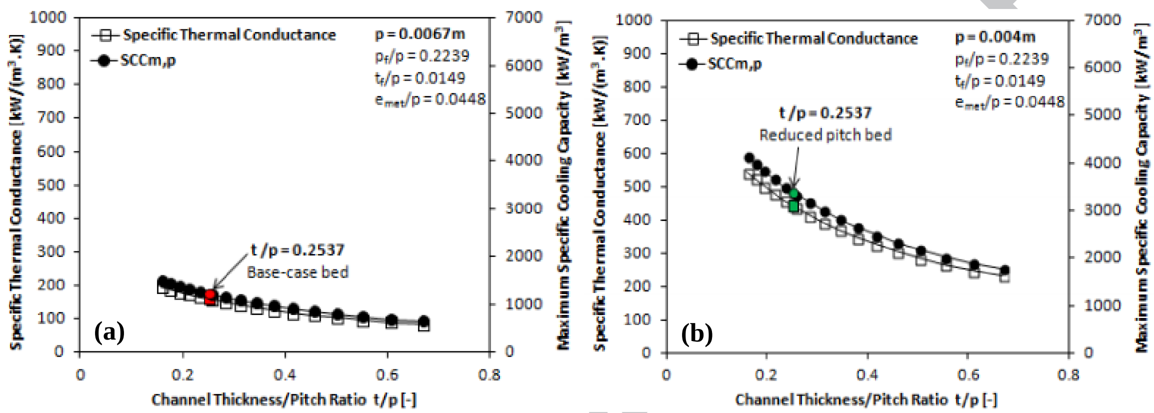

Fig. 9. Effect of t/p on specific thermal conductance and $SCC_{m,p}$ for: (a) Base-case bed: p=0.0067 m and (b) Reduced pitch bed: p = 0.004 m

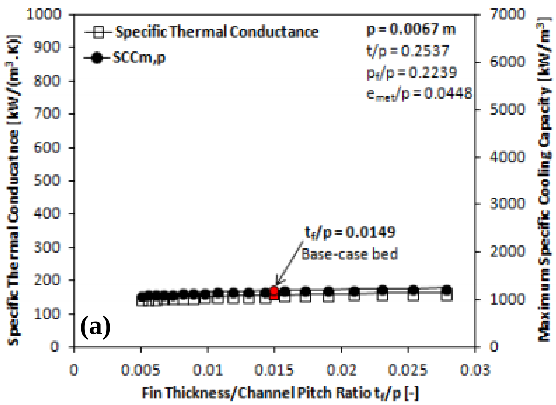

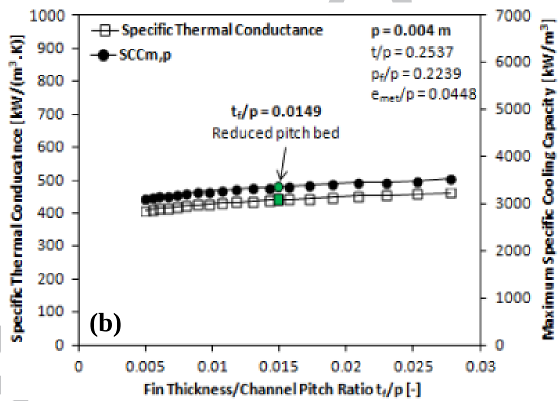

Fig. 10. Effect of t_f/p on specific thermal conductance and $SCC_{m,p}$ for: (a) Base-case pitch: p=0.0067 m and (b) Reduced pitch: p = 0.004 m

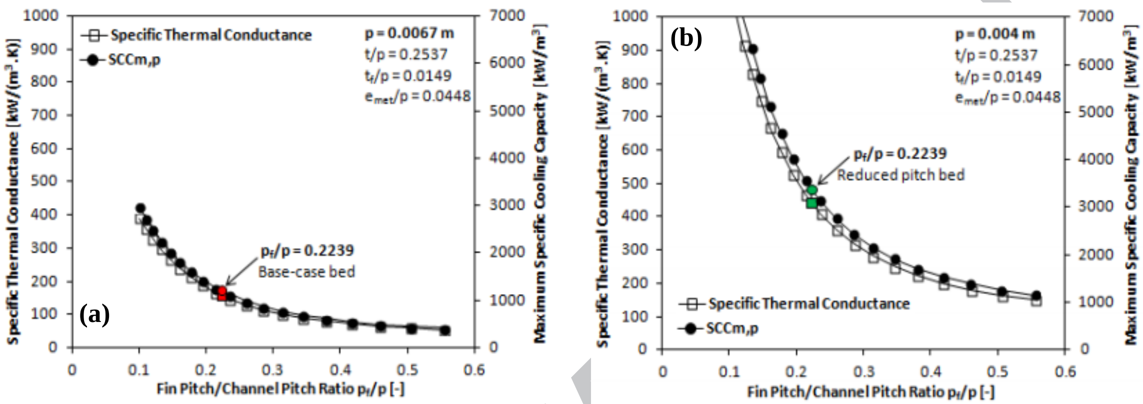

Fig. 11. Effect of p_f/p on specific thermal conductance and $SCC_{m,p}$ for: (a) Base-case pitch: p=0.0067 m and (b) Reduced pitch: p = 0.004 m

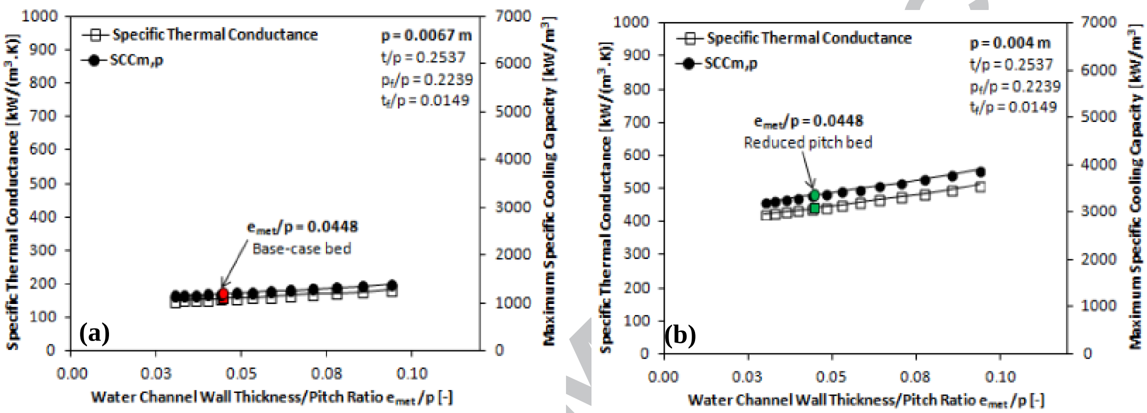

Fig. 12. Effect of e_{met}/p on specific thermal conductance and $SCC_{m,p}$ for (a) Base-case pitch: p=0.0067 m and (b) Reduced pitch: p = 0.004 m

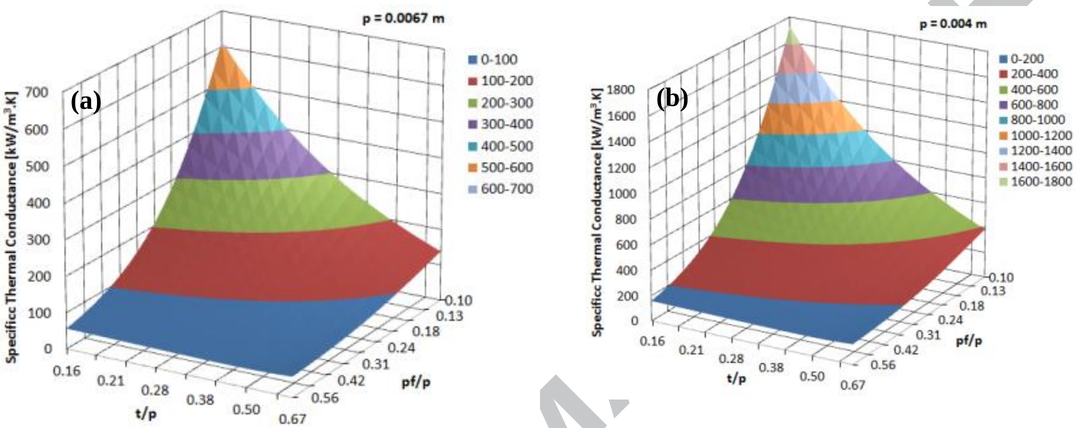

Fig. 13. Effect of t/p and p_f/p on specific thermal conductance for: (a) Base case bed: p=0.0067 m and (b) Reduced pitch: p = 0.004 m

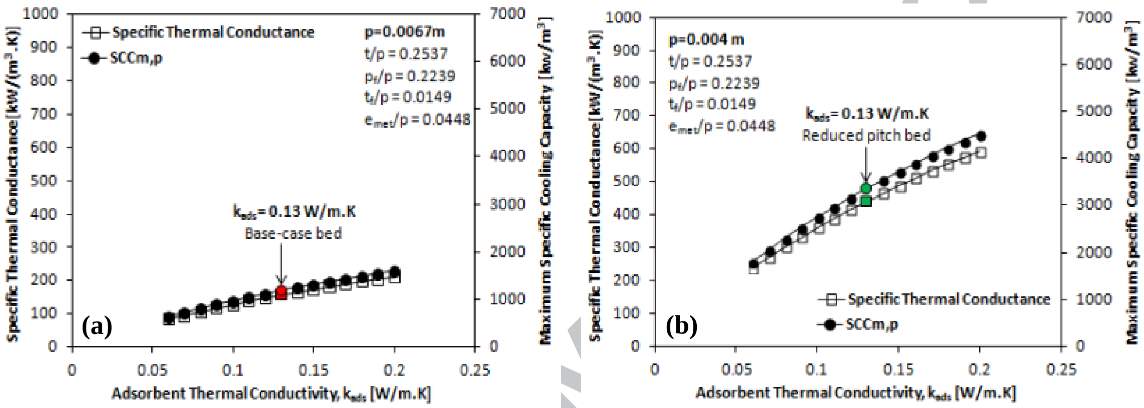

Fig. 14. Effect of k_{ads} on specific thermal conductance and $SCC_{m,p}$ for: (a) Base-case pitch: p=0.0067 m and (b) Reduced pitch: p = 0.004 m

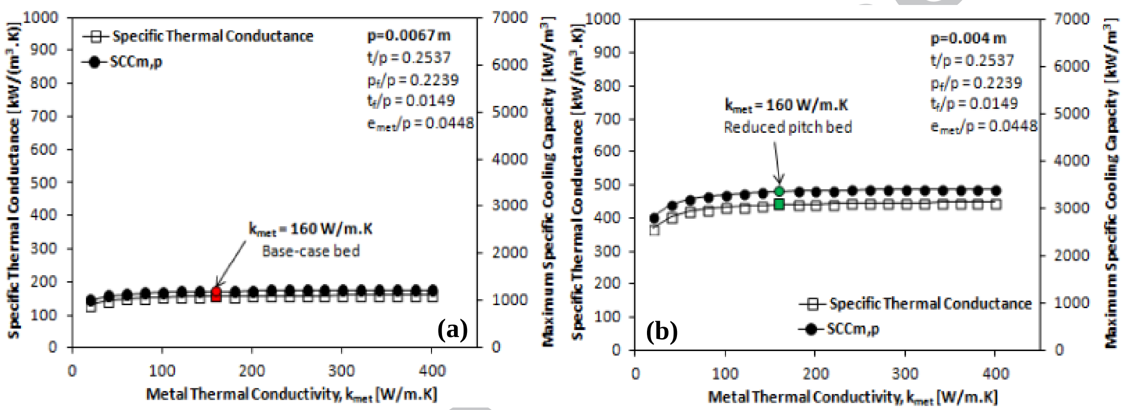

Fig. 15. Effect of metal thermal conductivity on specific thermal conductance and $SCC_{m,p}$ for: (a) Base-case pitch: p=0.0067 m and (b) Reduced pitch: p = 0.004 m

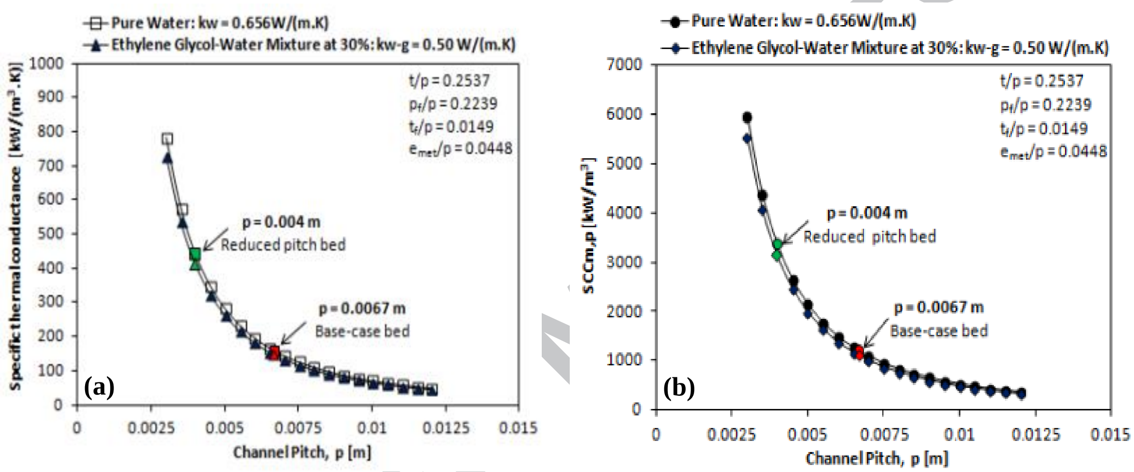

Fig. 16. Effect of the heat transfer fluid thermal conductivity on: (a) Specific thermal conductance and (b) $SCC_{m,p}$

Tables

Nomenclature			
A	area	R_{tot}	total thermal resistance, KW^{-1}
$A_{w,t}$	total heat transfer area for the water side, m^2	T	Temperature, ^oC
$COP_{m,p}$	maximum practical coefficient of performance	V	volume, m
COP_{max}	maximum theoretical coefficient of performance	V_{ch}	channel tube volume, m^3
cp	specific heat capacity, $Jkg^{-1}K^{-1}$	V_f	fin volume, m^3
$\overline{cp}_b$	equivalent heat capacity of the bed per adsorbent mass, JK^{-1}	W	wide, m
D	diameter, m	w	uptake, $kgkg^{-1}$
h	specific enthalpy, Jkg-1	**Subscripts**	
H	Height, m	ads	adsorbent
$h_{eq,1}$	unfinned surface equivalent convection heat transfer coefficient, $Wm^{-2}K^{-1}$	ch	channel tube
$h_{eq,2}$	finned surface equivalent convection heat transfer coefficient, $Wm^{-2}K^{-1}$	cond	condenser
L_f	fin length, m	des	desorption
m	mass, kg	evap	evaporator
$m_{met,tot}$	total metal mass in the heat exchanger (including headers), kg	f	fin
$m_{w,tot}$	total water mass in the heat exchanger (including headers), kg	met	metal
$m_{ads.b}$	total dry adsorbent mass per heat exchanger, kg	sat	saturated
$m_{met,HE}$	total metal mass per heat exchanger, kg	tot	total
$m_{ads,b}$	total mass of dry adsorbent packed in each bed, kg	w	water
$\dot{m}$	mass flow rate, kgs^{-1}	**Greek Letters**	
P	pressure, mbar	τ	half cycle time, s
$\dot{Q}$	total heat transfer rate, W	ρ	density, kgm^{-3}

Table 1. Base-case of the bed geometrical parameters

Parameter	**Symbol**	**Value**	**Unit**
Depth	D	0.038	m
Height	H	0.210	m
Wide	W	0.255	m
Channel pitch	p	0.0067	m
Flat tube thickness	t	0.0017	m
Fin pitch	p_f	0.0015	m
Fin thickness	t_f	0.0001	m
Water channel wall thickness	e_{met}	0.0003	m
Number of tube channels	N_{ch}	38	-

Table 2. Nominal operating conditions for the two-bed adsorption chiller.

Heating water in (heating water loop)		**Cooling water in (cond. + bed cooling loop)**		**Chilled water in (chilled water loop)**	
$T_{hw,in}$ [^{o}C]	$\dot{m}_{hw}$ [kgs^{-1}]	$T_{cw,in}$ [^{o}C]	$\dot{m}_{cw}$ [kgs^{-1}]	$T_{cw,in}$ [^{o}C]	$\dot{m}_{chw,in}$ [kgs^{-1}]
90	0.20	33	0.20	15	0.13

Total cycle time: 360 s

Table 3. Base-case thermal parameters

Parameters	Symbol	Values	Unit	Ref.
Water thermal conductivity at 61.5 °C	k_w	0.656	$Wm^{-1}K^{-1}$	[36]
Adsorbent thermal conductivity	k_{ads}	0.13	$Wm^{-1}K^{-1}$	[34]
Metal thermal conductivity of the bed	k_{met}	160	$Wm^{-1}K^{-1}$	[37]
Metal specific heat capacity	cp_{met}	890	$Jkg^{-1}K^{-1}$	[37]
Water specific heat capacity	c_{pw}	4182	$Jkg^{-1}K^{-1}$	[37]
Enthalpy of vaporization at 15 ºC	Δh_v	2465.7E03	Jkg^{-1}	-
Desorption enthalpy	Δh_{des}	3115.9E03	Jkg^{-1}	-

Table 4. Varied design conditions of adsorbent beds.

	Parameters	Symbol	Values	Unit
Geometrical	Channel pitch	p	3 - 12	mm
	Flat tube thickness /pitch ratio	t/p	0.16 - 0.668	-
	Fin thickness/ channel pitch ratio	t_f/p	0.005 - 0.0278	-
	Fin pitch/ channel pitch ratio	p_f/p	0.1 - 0.555	-
	Water channel wall thickness/ channel pitch ratio	e_{met}/p	0.0298 - 0.0936	-
Thermal	Adsorbent thermal conductivity of the bed	k_{ads}	0.06 - 0.20	$Wm^{-1}K^{-1}$
	Metal thermal conductivity of the bed	k_{met}	20 - 400	$Wm^{-1}K^{-1}$
	Heat transfer fluid thermal conductivity	k	0.5 - 0.656	$Wm^{-1}k^{-1}$
Mass	Metal/adsorbent mass ratio	$m_{met,tot}/m_{ads,HE}$	0.1 to 2.66	-
	Metal/adsorbent mass ratio	$m_{met,tot}/m_{ads,HE}$	0.1 to 2.66	-
Temp.	Heating water temperature	$T_{hw,in}$	70 - 120	ºC
	Cooling water temperature	$T_{cw,in}$	20 - 40	ºC
	Chilled water temperature	$T_{chw,in}$	5 - 20	ºC

Table 5. Adsorption properties of working pairs under study [34, 38].

Adsorbent-adsorbate pairs	**$cp_{ads,0}$ [$Jkg^{-1}K^{-1}$]**	**Δh_{des} [$kJkg^{-1}$]**	**w_{min} [$kgkg^{-1}$]**	**w_{max} [$kgkg^{-1}$]**	**Δw [$kgkg^{-1}$]**
Sorbsil A (silica gel) - water	750	3115.9	0.0205	0.1781	0.1576
SWS-1L (silica gel)- water	817	2610.4	0.1232	0.4554	0.3322
Zeolite 4A- water	980	7381.5	0.3449	0.3814	0.0365
FAM-Z02 (zeolite)- water	914	2795.1	0.0954	0.2996	0.2042

Highlights

- An analytical model was developed to determine the optimum geometrical and thermal parameters of a flat tube-fin adsorbent bed to obtain the maximum system performance.
- The overall thermal conductance of the bed and the maximum specific cooling capacity increased when reducing in flat tube thickness and fin pitch as well as by increasing in fin thickness and water channel wall thickness.
- The specific thermal conductance increased by 2.5% when reducing the channel pitch from its design value to a minimum permissible (0.004m).
- Adsorbent thermal conductivity is the most sensitive parameter to the specific thermal conductance in beds.
- The system performance significantly enhanced by reducing the mass of the metal bed and the heat transfer fluids as well as the desorption heat of the selecting working pair.